Saturated operation of a transient collisional x-ray laser

M. P. Kalachnikov,[1] P. V. Nickles,[1] M. Schnürer,[1] W. Sandner,[1] V. N. Shlyaptsev,[2] C. Danson,[3] D. Neely,[3] E. Wolfrum,[3] J. Zhang,[3] A. Behjat,[4] A. Demir,[4] G. J. Tallents,[4] P. J. Warwick,[5] and C. L. S. Lewis[5]

[1]*Max-Born-Institute, Rudower Chaussee 6, D-12489 Berlin, Germany*
[2]*P. N. Lebedev Physical Institute, 117924 Moscow, Russia*
[3]*Rutherford Appleton Laboratory, Chilton, Didcot, Oxfordshire OX11 0QX, United Kingdom*
[4]*Department of Physics, University of Essex, Colchester CO4 3SQ, United Kingdom*
[5]*School of Mathematics and Physics, Queen's University of Belfast, Belfast BT7 1NN, United Kingdom*
(Received 13 January 1998)

Saturation of a low pump energy x-ray laser utilizing a transient inversion mechanism on the $3p$-$3s$ transition at 32.63 nm in Ne-like Ti has been demonstrated. A close to saturation amplification was simultaneously achieved for the $3d$-$3p$, $J=1 \rightarrow 1$ transition at 30.15 nm. Small signal effective transient gain coefficients of $g \sim 46$ and ~ 35 cm^{-1} and gain-length products of 16.7 and 16.9 for these lines were obtained. Experiments demonstrate that it is possible to achieve saturated laser action in a transient regime with Ne-like Ti for a pump energy as low as ~ 5 J. [S1050-2947(98)09105-7]

Since x-ray lasing was first demonstrated in 1985 [1], much time and effort have been expended improving x-ray laser (XRL) efficiency and attempting to reduce its size and cost to make it attractive for potential users without access to large scale facilities. Numerous investigations were concentrated around optimization of different x-ray lasing schemes as well as methods of plasma creation. The notion ''table-top'' x-ray laser became a common expression for describing a scale acceptable for science and technology, for universities and small labs. At the present time, the ''traditional'' collisional x-ray lasers, for example, show gain-length product GL up to 12.5 at pump energy levels less than 300–400 J on several elements $Z=14$–31 [2]. In the last few years the investigations have shifted into the sub-100 J pump energy range [3]. This improvement of efficiency was achieved by mitigating refraction through the use of prepulses [4]. Since plasma based x-ray lasers require increasing pump power to generate shorter wavelengths, the development of new CPA ps and fs-pulse lasers is extremely important for x-ray laser development. Other pumping schemes became possible using these lasers, utilizing high electric field and different aspects of its influence on ion excitation [5]. Recombination-pumped lasers definitely benefited from shorter pulse duration, exhibiting $GL \sim 6$ at $\lambda \sim 18.2$ nm with just a 21 J, 2 ps pumping pulse [6]. One of the important steps on the route of improvement of efficiency was done with the collisional excitation scheme. X-ray lasing in Ne-like Ti with a gain coefficient of 19 cm^{-1} and a drastically reduced pump level of only a few Joules was demonstrated recently [7]. Following it, the Ni-like Pd with gain-length product of $GL \sim 12$ showed strong lasing at 147 Å [8]. These achievements were based on a novel collisional scheme, which was proposed some years ago [9] and then developed theoretically by several authors [10–12]. All these small pump energy experiments were promising, but the saturation limit, resulting in extraction of a substantial part of the stored energy, was not reached in them. To date, the only table-top x-ray laser, which surpassed the saturation point, is Ne-like argon at 46.9 nm (with up to ~ 30 μJ energy in double-pass amplification geometry, ~ 800 ps duration) using a fast capillary discharge plasma, which is a kind of Z-pinch device [13]. With this work we report the achievement of x-ray laser saturation in a laser plasma-based x-ray laser, with extremely low pump requirements of several Joules. It is shown that this opens the route to saturated x-ray lasing in Ne-like titanium in a table-top implementation.

The scheme is based on creation of a plasma containing the desired active ions (for example, neonlike, nickel-like, etc., though it potentially works with almost all other ions) by a preliminary laser pulse irradiating a target, followed by a short (ps) pulse that heats the preformed plasma. Due to the fast collisional excitation, a transient population inversion occurs [9,11] within a short time period. This is due to the different population rates of the lasing energy levels, in contrast to the collisional-radiative depopulation of the lower laser level relevant to the quasi-steady-state (QSS) regime. The transient inversion is characterized by a short lifetime and yields much higher gain coefficient values (~ 100 cm^{-1}) than can be obtained in the QSS regime (several cm^{-1}) with relatively long pulse pumping. Note that due to the very high values of transient gain coefficient, its contribution may be substantial even in experiments where the QSS approach is expected to dominate. Since the transient inversion is a property of the atomic kinetics, it can be realized in very different plasma conditions. For example, the contribution due to transient effects was calculated to be up to $\sim 30\%$ in a recently realized capillary discharge x-ray laser operating at 60.5 nm in Ne-like sulfur [14]. Together with large gain values, the short lifetime of the transient inversion opens the possibility to operate x-ray lasers at 100–1000 Å with a very low pump energy requirement of several Joules or less. The experimental demonstration of saturation in the transient inversion concept is an important step, which in all cases will be hard or even impossible to achieve. Its demonstration here for transient mechanism is encouraging for the development of tabletop x-ray lasers and provides a new route to shorter x-ray wavelengths.

The possibility of saturating Ne-like Ti using the long and short pulse pumped transient excitation scheme was noted in [7,11], but fully saturated operation was not observed. Small gain-length products ($GL<9$) have been observed in other long pump pulse collisional (QSS) Ti lasers at 32.63 nm but lasing on the $3d$-$3p$ line ($\lambda=30.15$ nm) of Ti has not been observed before in the quasi-steady-state regime [5,15], though in this regime some amplification with $GL\sim3-4$ has been observed in Ne-like Ar [16].

As shown in our previous publication [7], the x-ray laser intensity as a function of laser length in the transient case may resemble a saturation curve when real saturation is actually not achieved. Besides the usual refraction effects, the rapid decrease of gain during the photon transit time along the medium can cause saturationlike behavior of exit radiation. In this work, we utilize several independent methods to provide reliable proof of real saturation. The amplification characteristics of the $3p$-$3s$ ($J=0\rightarrow1$) transition at $\lambda=32.63$ nm and the $3d$-$3p$ ($J=1\rightarrow1$) transition at $\lambda=30.15$ nm have been studied with the wider range of laser heating parameters (3–21 J) and extended plasma column lengths (up to 10 mm). This enabled us to determine gain-length products from the experiment with substantial accuracy (as compared to [7]) as the proof of saturation. A second independent method came from the comparison of the relative intensities of the two lasing lines ($\lambda=32.63$ and 30.15 nm), and is based on higher saturation intensity for the latter line. It was found experimentally that the relative intensities of these lines provide strong evidence of saturation. Third, agreement between calculated and measured absolute values of extracted energy provides additional evidence of saturation. Besides the questions of saturation, the dependence of the x-ray laser output energy on the optical laser pump energy was measured, which allowed us to find optimum efficiency pump values. The x-ray beam divergence and pointing direction was also determined, which enabled us to define the value of the optimum electron density at which the titanium transient x-ray laser operates.

The experiments were carried out with the Rutherford Appleton Laboratory Vulcan Nd:glass laser, using a CPA-laser beam [17] capable of delivering up to 40 J laser energy (E_L) with a pulse width of several picoseconds (2–3 ps at low E_L and 6–8 ps at high E_L) and a second synchronized ns-laser beam of several tens of Joules. In "standard" experimental conditions we have used an energy density of 1.7 J/mm in the long pulse ($\sim1.7\times10^{12}$ W/cm^2 for ~1 ns pulse) and of 1.5 J/mm in the short pulse (i.e., $\sim2.2\times10^{14}$ W/cm^2 for ~7 ps pulse). The short pulse was timed at the falling edge of the long 1 ns pulse which had a flat top temporal profile. The line foci of the two beams, with a common overlap length of 10 mm and a width of 100 μm, were superimposed on the target. Due to the astigmatic irradiation geometry of the short pulse beam, a running focus with a phase speed of about two and a half times the speed of light was always present in the direction towards the spectrometer slit. Ideally, a speed of light running focus is required, and it will be the subject of future investigations.

Titanium stripes, with a thickness between 0.6 and 1.0 μm and a width of about 210–300 μm, coated on glass substrates and massive slab Ti targets, were both used in this experiment but there were no obvious differences in perfor-
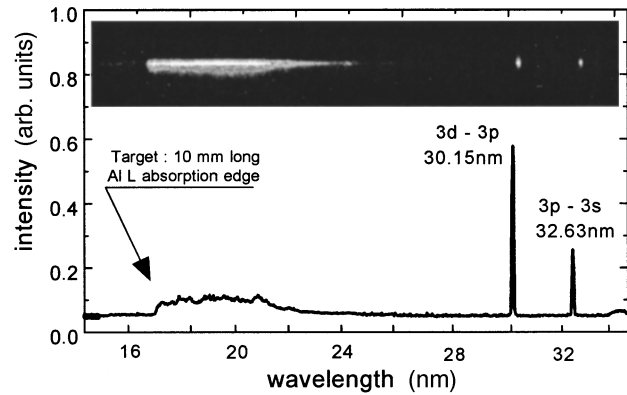
FIG. 1. Spectral characteristics of the transient inversion collisional x-ray laser in Ne-like Ti. The spectrum is not corrected for transmission of an Al filter (3μ) used in front of the CCD camera.

mance. The active medium length was varied by choosing targets of different length. The primary diagnostic, viewing along the target axis, was a flat field grazing incidence XUV spectrometer with an aperiodically ruled grating. Focusing perpendicular to the dispersion direction was provided by a cylindrical mirror. The time integrated spectrum was recorded with a back-thinned, XUV sensitive, 16 bit CCD camera. For high x-ray laser signals Al filters were used in front of the spectrometer to prevent saturation of the CCD camera. The corresponding absorption values were taken into account to estimate the lasing signal intensity.

The typical spectral characteristics of the Ti Ne-like transient inversion x-ray laser are shown in Fig. 1. One can see that two spectral lines corresponding to the $3p$-$3s$ ($J=0\rightarrow1$) and $3d$-$3p$ ($J=1\rightarrow1$) transitions in Ne-like Ti dominate the emission spectrum. Lasing on both spectral lines in the transient regime was observed previously [7], but because of poor spectral resolution and weak intensity we were not able to determine the wavelength of the $3d$-$3p$ transition or its gain coefficient. We estimate that the spectral resolution of the wavelength-calibrated spectrograph used in the current experiments was 0.05 nm, and we are able to evaluate the wavelength of the $3d$-$3p$ lasing transition ($J=1\rightarrow1$) in Ne-like Ti. It has an experimental value of $\lambda=(30.15\pm0.05)$ nm. It is worth noting that lasing on this transition in Ne-like Ti laser plasmas using the QSS regime has never been observed, though in this regime some amplification with $GL\sim3-4$ has been observed in Ne-like Ar [16].

The output from the two spectral lines varies differently with target length (see Fig. 2.). The $3d$-$3p$ line is rather weak at short target lengths, becomes nearly as bright as the $3p$-$3s$ line at target lengths of ~7 mm, and can exceed the output of the $3p$-$3s$ transition at long target lengths. At long target lengths (10 mm) the energy emitted in each of the spectral lines approaches ~21 and ~25 μJ for $3p$-$3s$ and $3d$-$3p$ lines, which surpasses the value corresponding to saturation intensity of the $3p$-$3s$ transition by approximately 1.8 times.

Analyzing the XRL output data given in Fig. 2 one can see that the XRL output for neither the $3p$-$3s$ transition ($\lambda=32.63$ nm) nor the $3d$-$3p$ transition can be fitted with the Linford [18] fit using a unique gain coefficient value within
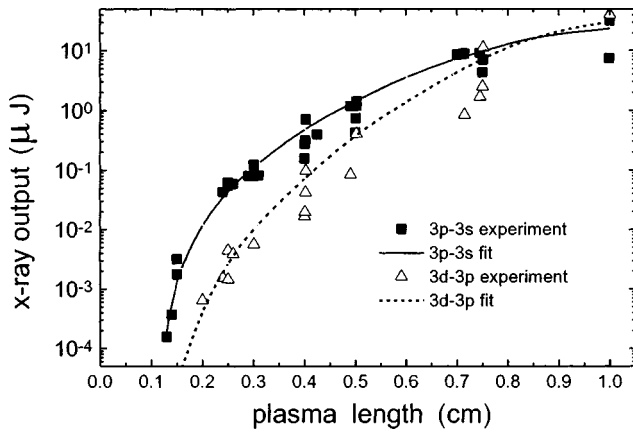
FIG. 2. Output signals of the x-ray laser at 32.63 nm (■) and 30.15 nm (△) as a function of target length for pump energies of 1.5 J/mm for the long and 1.7 J/mm for the short pulses, respectively. The solid and dotted lines are corresponding fits.

the whole range of target lengths used (1–10 mm). Smooth curves drawn on Fig. 2 represent the growth curves for the best shots recorded for each lasing line and the slope of these curves is used to find a local or effective gain coefficient. The transient gain contribution is clearly pronounced at small target lengths up to $L \sim 3$ mm, where effective gain coefficients are determined as $g \sim 46$ cm^{-1} and $g \sim 35$ cm^{-1}, for the 32.63 and 30.15 nm lines, respectively. Calculations show that peak local gain coefficients (i.e., maximum values in space and time) are about 1.5–2 times higher in the density regions through which amplifying rays propagate [7,21]. As the target length increases the rate of increase of the output signals drops, indicating a falling effective gain coefficient. There are several reasons which explain these effects.

Some results of x-ray laser modeling with the code RADEX [9,22,23] for the case of typical experimental illumination conditions are presented in Fig. 3. There are two regions in
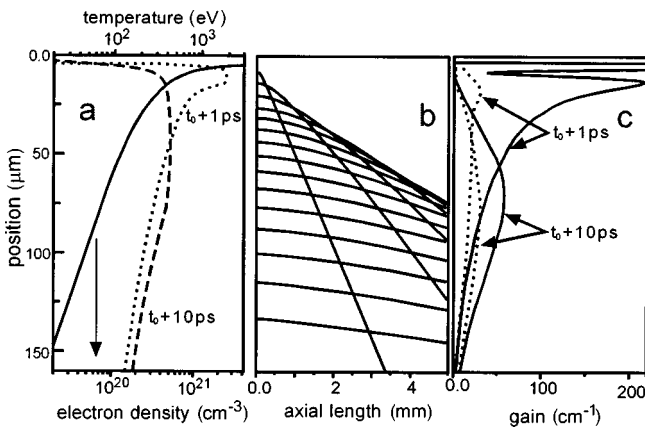
FIG. 3. Results of RADEX transient inversion x-ray laser modeling for Ne-like Ti and typical illumination conditions (1.7 J/mm in the long pulse and 1.5 J/mm in the short pulse). Distributions of hydrodynamic plasma parameters: density (solid curve) and temperature (dashed and dotted curves) (a); ray trajectories of $3p$-$3s$ lasing rays (b); distribution of transient (solid curves) and QSS (dotted curves) gain for different time moments, where t_0 corresponds to the moment of the short pulse arrival (c).

the plasma density profile which exhibit very high gain values. They are undercritical ($n_e < 10^{21}$ cm^{-3}) and overcritical ($n_e > 10^{21}$ cm^{-3}) regions. The gain increases in the overcritical region of plasma since the heat wave forms a front moving in dense ablative material, where (in a narrow region) the gain reaches very high values. This gain exists locally during a very short time interval < 1 ps and then disappears. The rays emitted from this region of plasma, because of strong refraction [Fig. 3(b)], leave rapidly the area of high gain values and hence do not give a significant contribution to the experimentally measured signal. The line broadening due to collisions and shortening of transient relaxation time are limiting the optimal densities to smaller values. Finally, the gain values also drop down rapidly in the vicinity of the critical density since the plasma temperature and density are high enough to overionize Ne-like ions. This explains why the local gain values in the calculations reach very high values, exceeding ~ 300 cm^{-1} near the critical density [Fig. 3(c)], but the most favorable amplification region lies in the density range $n_e \sim (1.5-2.5) \times 10^{21}$ cm^{-3}, which is close to the optimal for the QSS regime too at these high temperatures. In the undercritical region the plasma corona is heated up to 400–500 eV by inverse bremsstrahlung and partially by the strong heat flux from the hot 2–3 keV region of critical electron density. The calculations suggest that the gain lifetime at $n_e \sim 2 \times 10^{21}$ cm^{-3} lasts ~ 10 ps. Taking into account the photon transit time of 10 ps through 3 mm of plasma, this time duration corresponds to the plasma lengths when the observed deviation from very fast exponential output signal growth becomes obvious (Fig. 2).

The measurements of beam divergence and pointing were done using targets of different lengths (5 and 9 mm) and different durations of the long pulse. The smallest divergence of 2–3 mrad was measured for both $3d$-$3p$ and $3p$-$3s$ transitions using 9 mm-long Ti-stripe targets and 0.6 ns long first pulses. It increased to 6–8 mrad for the 1-ns-long prepulse. The pointing in both cases was within $\phi = 8-9$ mrad. When the active medium length is 3–4 times longer than the refraction length $L_r = d/\phi \sim 1$ cm [24], where $d \sim 0.01$ cm is the plasma size, the optimum x rays emerge from the rear of the plasma outside the maximum gain region [see Fig. 3(b)]. In this case the tilt angle does not depend on the plasma gradients and can be defined by the optimum density using the relation $\phi = (n_e/n_{c\lambda})^{0.5}$, where $n_{c\lambda}$ is the critical density for the x-ray laser frequency (1.06×10^{24} cm^{-3} and 1.24×10^{24} cm^{-3}, respectively). In our case of relatively short plasma the x-ray flux emerged from the active medium at radii ~ 0.01 cm, where the electron density remains high $(0.5-1) \times 10^{21}$ cm^{-3} [Figs. 3(a) and 3(b)]. It was found experimentally that both $3p$-$3s$ and $3d$-$3p$ spectral lines are emitted in almost the same plasma regions, which is confirmed by very close values of their pointing angles and divergence. In this case the influence of refraction, temperature, etc. on both x-ray lasing lines should be nearly the same. There are similarities and some differences in the nature of the transient inversion for these lines. They are both excited by direct electron collisions from the ground state. A specific property of inversion on the $3d$-$3p$ transition is its direct dependence on reabsorption of the $3d$-$2p$ radiative depopulating transition, while the $3p$-$3s$ one is substantially less affected by this process, via electron collisions between

$3p$ and $3d$ states. Also lower laser level populations for the $3p$-$3s$ laser transition are directly affected by the reabsorption of the $3s$-$2p$ line, while for the $3d$-$3p$ laser transition this takes place indirectly through the intermediate stage of collisions between its lower laser level $3p$ and $3s$ states. Note that strong $3d$-$2p$ radiative trapping always takes place due to its large absorption oscillator strength (~ 2.6 and the largest in Ne-like ions), and hence keeps the $3d$ population much higher than in the optically thin limit. Inversion on these transitions in QSS plasma was calculated in [19,20]. It was shown that the gain in almost all x-ray lasing transitions is affected (in a negative or positive way) by reabsorption (or radiative trapping, or, according to [20], self-photopumping). In the transient regime, the inversion on this transition is defined by the rate of direct excitation of the $3d$ level (the strongest in Ne-like ions), while the $3p$ level is excited much more slowly. Hence, in contrast to the QSS regime, the transient inversion here exists in both optically thin and optically thick limits but in the latter case can approach that of the $3p$-$3s$ transition [7,20,21].

Strong decay of the $3d$ level causes one very important property for $3d$-$3p$ laser generation. We found by numerical modeling that the contribution of natural and collisional broadening to this transition, related to the strong $3d$-$2p$ radiative decay and numerous collisional cascades, causes the $3d$-$3p$ saturation intensity to be ~ 2.8 times larger than the $3p$-$3s$ transition saturation intensity at noted densities, while source functions for both transitions differ by less than 21%. Due to this remarkable difference in saturation intensities and their very close wavelengths and similar amplification densities, we used their intensities as one of the most reliable proofs of saturation. Atomic kinetics calculations by RADEX give the following saturation intensities for $3p$-$3s$ and $3d$-$3p$ transitions: 1.18×10^9 W/cm^2 and 3.15×10^9 W/cm^2 respectively. A clear indication of the $3p$-$3s$ transition saturation is the fact that the output and GL product (see below) for the $3d$-$3p$ line becomes larger than for the $3p$-$3s$ line at longer target lengths. For comparison, in the MBI experiment [7] for which RADEX predicted a gain-length product of $GL \sim 15.5$ at saturation, the $3d$-$3p$ line was ~ 7 times weaker than the $3p$-$3s$ one.

The dependence of the gain coefficient on target length can be estimated from local Linford fits to the data points presented in Fig. 2. Note that the output signal from active lengths shorter than $L \leqslant 1.5$ mm was not measured, but taking into account that for these small target lengths the effective gain coefficient values are not affected by transit time effects or refraction, and thus approach the local plasma gain coefficient values defined by atomic kinetics, we have estimated the effective gain-length products over the full range of target lengths. These dependencies are presented in Fig. 4. As can be seen from Figs. 2 and 4, the phase of transient gain formation in the interval of the first 10 ps, or the first 3 mm of plasma length, gives the largest contribution to the GL product. With the longest target lengths of 10 mm, maximum values of $GL = 16.7$ and $GL = 16.9$ were achieved, respectively, on the $3p$-$3s$ and $3d$-$3p$ transitions. Calculations suggest GL at saturation of 16–16.2 and 17.1–17.4 for these lines. It is worth noting that the $3d$-$3p$ line in our experimental conditions was very close to the saturation limit, which could be achieved at about 1.1–1.2 cm of plasma
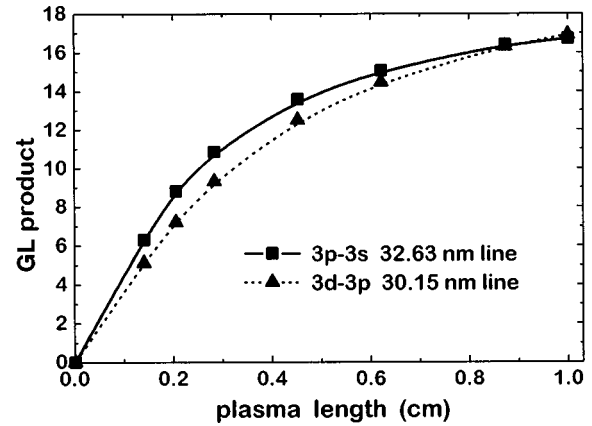
FIG. 4. Dependence of the effective gain-length product on the target length. The curve shows how the effective gain-length product increases with target length, reaching for the $3p$-$3s$ transition the value of $GL = 16.2$ related to saturation at the target length of ~ 8.3 mm.

length compared to 8–8.3 mm for the $3p$-$3s$ line. Finally, it is interesting that a simple estimate based on geometrical considerations [24] gives $GL = \ln[(4\pi/\Omega)(\Delta\omega/\Delta\omega_g)(\Delta N/N_u)q]$, where Ω is a solid angle ($\Omega \sim 2 \times 10^{-4}$ and 1.4×10^{-4} for the $3p$-$3s$ and $3d$-$3p$ lines, respectively), $\Delta\omega$ and $\Delta\omega_g$ are linewidths of emission and laser generation [$\Delta\omega/\Delta\omega_g \sim (GL)^{0.5}$], ΔN and N_u are inversion and upper laser level populations ($\Delta N/N_u \sim 0.5$), and q is a quenching parameter at saturation (~ 70 and ~ 144 for the $3p$-$3s$ and $3d$-$3p$ lines, respectively). This gives for these lines the following criteria for saturation: $GL = 16.1$ and 17.1. Due to the very slow logarithmic dependence on the parameters, this estimate is within 15% of more complex numerical calculations by RADEX. The estimate is based on the local plasma gain and hence serves as an upper limit for the saturated GL requirement [13,24]. All experimentally measured GL values, obtained utilizing local fits by the Linford formula, which provide the effective gain, already include all detrimental influences such as refraction, inhomogeneities, short transient nature of the gain, etc. This analytical estimation, being close to the experimental values, serves as a clear supplemental indication that saturation has been achieved.

Another important feature of our experiment was an investigation of the role of the traveling wave illumination in transient x-ray laser experiments. Due to the special irradiation geometry of the short pump pulse, the focal point had an intrinsic velocity along the plasma column with a phase speed of $\approx 2.5c$ in the direction towards the spectrometer (''natural'' traveling wave). This running focus was slowed to the speed of light (c) by inserting a diffraction grating in the CPA beam line, which introduced a shear across the wave front. The resulting traveling wave velocity in the target plane was verified experimentally using an ultrafast optical streak camera. At the present time, due to data scatter and an insufficient number of experimental points, no quantitative comparison of the effective gain and GL can be made between the natural and ideal traveling wave cases. However, no systematic difference could be found in the output lasing signals with or without the diffraction grating in place, though there were several shots. This shows that the gain duration was a significant fraction of the 33 ps transit time of a 10 mm target, consistent with RADEX modeling, which suggests that gain consists of a combination of transient and, in
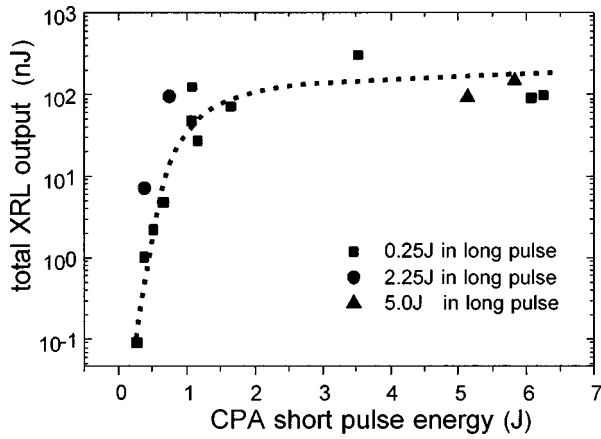
FIG. 5. Dependence of the XRL output ($3p$-$3s$ transition in Ne-like Ti) on the pump energy in the short pulse for different values of the long pulse energy. Targets of 3 mm length were used. The experimental dependence shows that increasing the energy from $E_{short} \approx 1.5$ J in a short laser pulse (corresponding energy deposition on the target of 0.5 J/mm) does not give a significant growth of the output XRL signal.

the late stage, some QSS contributions. For clarity, only data recorded with the ''natural'' traveling wave (i.e., with the grating removed) are included in Fig. 2.

One of the most important issues studied is related to the pump energy consumption. In a second series of experiments we determined the pump energy values essential for lasing at 32.63 nm. We choose 3 mm targets and changed energy in both the short as well as in the long pulse. Using either the short or long pulse alone, no lasing was visible with the maximum energy values used in this experiment. Pump energies on a 3 mm target as low as $E_{long} = 0.25$ J and $E_{short} = 0.25$ J yield measurable amplified emission. With $E_{short} \approx 1.5$ J one achieves already the maximum XRL signal output in this pumping scheme (see Fig. 5). An increase of the long pulse intensity up to a factor of 21 did not give a higher output signal providing E_{short} was greater than 1.5 J. With $E_{short} = 1.5$ J for the short pulse (i.e., 0.5 J/mm or an intensity of $I_s = 1.7 \times 10^{14}$ W/cm^2 in a 3 ps pulse) and $E_{long} = 0.25$ J for the long pulse (i.e., 0.08 J/mm or an intensity of 8.3×10^{10} W/cm^2 in a 1 ns pulse) we observed the same XRL output signal as presented in Fig. 2, for a 3 mm target. This indicates that a gain-length product of 10.5–11 was achieved in these conditions. This verifies that x-ray lasing in the Ne-like Ti system is possible with table top class pump lasers. We note that within the threshold region ($E_{short} < 1.5$ J) the lasing output was sensitive to the energy in the long pulse.

According to calculations, 0.25 J in the long pulse heats the plasma up to 70–80 eV and gives 50–60 % of ions in the Ne-like state. It is well known that Ne-like ions are present in plasma through a wide range of temperature. For Ti XIII this range is from 70 eV up to 150 eV in a steady-state regime and up to 210 eV in our quasi-steady-state conditions during the ns pulse. A 3–5 times increase of long pulse energy results, according to RADEX (or just a simple analytical model [23]) in an increase of initial temperature to the optimal range of 140–180 eV. This explains such a wide range of suitable long ns-pulse laser energies. The short laser pulse energy range is also relatively wide because after it exceeds the level ~ 1.5 J, which causes a temperature jump $T_e \sim E_u$ in the preformed plasma, the excitation rate does not increase further but decreases logarithmically slowly with increasing T_e [9]. Similar tendencies are exhibited in the QSS inversion, which follows the transient inversion after relaxation of the level populations [9]. Note that despite the uniquely low pump energy requirements obtained in this work, there may exist potentially more efficient plasma hydrodynamic methods, for example, utilizing low density targets or some other techniques [25]. We will address these issues in our future investigations.

In summary, our transient inversion collisional excitation scheme results in reliable x-ray lasing of the $3p$-$3s$ transition at 32.63 nm with very low pump energy consumption (0.5 J/mm for a ps laser pulse) corresponding to table top requirements. Saturation of the lasing signal in this excitation regime is demonstrated. A very high transient gain coefficient $g > 46$ cm^{-1} for the $3p$-$3s$ ($J = 0 \to 1$) transition in Ne-like Ti was obtained. A gain coefficient value $g \sim 35$ cm^{-1} for the $3d$-$3p$ ($J = 1 \to 1$) lasing line in Ne-like Ti was also measured, and amplification very close to saturation observed. The wavelength of this spectral line was determined as (30.15 ± 0.05) nm. Finally, with output energies of about 21 and 25 μJ for the $3p$-$3s$ and $3d$-$3p$ lines, corresponding to an energy efficiency of 2×10^{-6}, the attraction of a new excitation scheme is demonstrated by this Ne-like Ti x-ray laser.

[1] D. L. Matthews *et al.*, Phys. Rev. Lett. **54**, 110 (1985); S. Suckewer *et al.*, *ibid.* **55**, 1753 (1985).

[2] Y. Li, G. Pretzler, P. Lu, E. E. Fill, and J. Nilsen, Phys. Plasmas **4**, 479 (1997).

[3] A. Prag, A. Glinz, J. E. Balmer, Y. Li, and E. Fill, Appl. Phys. B: Lasers Opt. **63**, 113 (1996).

[4] T. Boehly *et al.*, Phys. Rev. A **42**, 6962 (1990), J. Nilsen *et al.*, *ibid.* **48**, 4682 (1993); E. E. Fill *et al.*, Proc. SPIE **2521**, 134 (1995).

[5] S. Suckewer *et al.*, J. Phys. (Paris), Colloq. **47**, C6-23 (1986); C. W. Clark *et al.*, J. Opt. Soc. Am. B **3**, 371 (1986); N. H. Burnett and P. B. Corkum, *ibid.* **6**, 1195 (1989); P. Amendt

et al., Phys. Rev. A **45**, 6761 (1993); B. E. Lemoff *et al.*, Opt. Lett. **19**, 569 (1994); Y. Nagata *et al.*, Phys. Rev. Lett. **71**, 3774 (1993); B. E. Lemoff *et al.*, *ibid.* **74**, 1574 (1995); B. N. Chichkov *et al.*, Phys. Rev. A **52**, 1629 (1995); D. V. Korobkin, C. H. Nam, A. Goltsov, and S. Suckewer, Phys. Rev. Lett. **25**, 5216 (1996).

[6] J. Zhang *et al.*, Phys. Rev. Lett. **74**, 1335 (1995).

[7] P. V. Nickles, V. N. Shlyaptsev, M. P. Kalachnikov, M. Schnürer, I. Will, and W. Sandner, Phys. Rev. Lett. **78**, 2748 (1997).

[8] J. Dunn, A. L. Osterheld, R. Shepherd, W. E. White, V. N. Shlyaptsev, and R. E. Stewart, Phys. Rev. Lett. **80**, 2825 (1998).

[9] Y. V. Afanasiev and V. N. Shlyaptsev, Sov. J. Quantum Electron. **19**, 1606 (1989).

[10] L. B. DaSilva *et al.*, Proc. SPIE **1229**, 128 (1990); M. D. Rosen and D. L. Matthews, US Patent No. 5016250 (1991); S. Maxon *et al.*, Phys. Rev. Lett. **70**, 2285 (1993); K. G. Whitney *et al.*, Phys. Rev. E **50**, 468 (1994).

[11] V. N. Shlyaptsev, P. V. Nickles, Th. Schlegel, M. P. Kalachnikov, and A. L. Osterheld, Proc. SPIE **2112**, 212 (1993).

[12] S. B. Healy, K. A. Janulewicz, J. A. Plowes, and G. J. Pert, Opt. Commun. **132**, 442 (1996).

[13] J. J. Rocca, D. P. Clark, J. L. A. Chilla, and V. N. Shlyaptsev, Phys. Rev. Lett. **77**, 1476 (1996).

[14] F. G. Tomasel, J. J. Rocca, and V. N. Shlyaptsev, Phys. Rev. A **55**, 1437 (1996).

[15] J. Zhang *et al.*, Phys. Rev. A **53**, 3640 (1996).

[16] H. Fiedorowicz, A. Bartnik, Y. Li, P. Lu, and E. Fill, Phys. Rev. Lett. **76**, 415 (1996).

[17] C. N. Danson *et al.*, Opt. Commun. **103**, 392 (1993).

[18] G. J. Linford *et al.*, Appl. Opt. **13**, 397 (1974).

[19] A. V. Vinogradov and V. N. Shlyaptsev, Sov. J. Quantum Electron. **13**, 303 (1983).

[20] J. Nilsen, Phys. Rev. A **55**, 3271 (1997).

[21] V. N. Shlyaptsev, J. J. Rocca, P. V. Nickles, M. P. Kalachnikov, and A. L. Osterheld, in *Proceedings of the International Conference ''X-ray Lasers,'' Lund, Sweden, 1996* (IOP, Bristol, 1996), Vols. 151 and 215.

[22] A. V. Vinogradov and V. N. Shlyaptsev, Sov. J. Quantum Electron. **19**, 1606 (1989); V. P. Avtonomov *et al.*, J. Sov. Laser Res. **10**, 1 (1989).

[23] A. V. Vinogradov and V. N. Shlyaptsev, Sov. J. Quantum Electron. **13**, 1511 (1983).

[24] V. N. Shlyaptsev, Ph.D. thesis, P. N. Lebedev Phys. Institute, Moscow (1987); R. London, Phys. Fluids **31**, 184 (1988).

[25] V. N. Shlyaptsev and A. Gerusov, *Proceedings of 3-d International Colloquium on X-ray Lasers, Schliersee, Germany* (IOP, Bristol, 1992), p. 195.